Theoretical Study of the Gas-Phase Reaction of Diborane(3) Anion $B_2H_3^-$ with CO_2

Zheng-wang Qu, Ze-sheng Li,* Yi-hong Ding, and Chia-chung Sun

State Key Laboratory of Theoretical and Computational Chemistry, Institute of Theoretical Chemistry, Jilin University, Changchun 130023, P. R. China

Received: June 12, 2000; In Final Form: August 30, 2000

The complex potential energy surface for the gas-phase ion−molecular reaction of the diborane(3) anion $B_2H_3^-$ with CO_2, including 12 $[B_2H_3CO_2]^-$ intermediate isomers and 17 interconversion transition states, has been investigated theoretically at the B3LYP/6-311++G(d,p) and single-point CCSD(T)/6-311++G(d,p) levels. The CCSD(T) calculations show that for the $B_2H_3^-$ anion the single-H-bridged isomer $HB(H)BH^-$ is thermodynamically 4.7 kcal/mol lower in energy than the kinetically rather unstable nonbridged isomer H_2BBH^-. The thermodynamical and kinetical stability of these $[B_2H_3CO_2]^-$ isomers are determined, and the possible reaction pathways leading to five low-lying dissociation products **(A)** $H_3BBO^- + CO$, **(B)** c-$BH_2OBH^- + CO$, **(C)** $H_2BCO^- + HBO$, **(D)** $H_3BCO + BO^-$, and **(E)** c-$BH_2OCH + BO^-$ are probed. It is shown that this reaction is initialized by the nucleophilic attack of $B_2H_3^-$ toward CO_2, and all the five products are both thermodynamically and kinetically accessible. Our calculated results for the gas-phase reaction of the $B_2H_3^-$ anion with CO_2 are in good agreement with the recent experimental results of Krempp et al., and may be helpful for understanding the chemical behavior of electron-deficient boron hydride anions.

1. Introduction

The boron chemistry has received much interest of chemists since the discovery of the first boranes in 1912 by Stock et al.[1] However, this area of chemistry is not yet nearly as developed as organic chemistry. Attempts to predict with a sufficient reliability the chemical behavior of a given compound, or to carry out a controlled synthesis of desired compound, only succeed relatively rarely. Our understanding of the chemical behavior and reaction mechanism of electron-deficient boron compounds is still inadequate.[2]

Recently, Krempp et al.[3] have investigated the gas-phase ion chemistry of boron hydride anions using the flowing afterglow selected-ion flow tube (FA-SIFT)[4] techniques. A host of new boron hydride anions such as $B_2H_3^-$, $B_3H_6^-$, $B_4H_7^-$, $B_5H_8^-$, and $B_{10}H_{14}^-$ are produced using the FA-SIFT and collision-induced dissociation (CID)[5] techniques. Several boron hydride anions that are known in solution[2] or have been produced previously in an ion cyclotron resonance (ICR) experiment[6] (e.g., BH_4^-, $B_2H_5^-$, $B_2H_7^-$, $B_3H_8^-$, $B_4H_9^-$, and $B_{10}H_{13}^-$) are also observed. Their reaction chemistry has been investigated[3] under thermal conditions with a variety neutral molecules including CO_2, COS, CS_2, pyrrole, *tert*-butyl alcohol, and other deuteration reagents such as D_2O, CH_3OD, and CH_3CO_2D. These reactions reveal a rich chemistry of boron hydride anions and may provide useful information for understanding the chemical behavior of electron-deficient boron compounds.

The $B_2H_3^-$ anion is particularly appealing for theory because it is one of the simplest electron-deficient boron hydride anions that may exhibit structural isomerism. For its neutral isoelectronic partner B_2H_4,[7] Stanton et al.[8] have predicted that the double-H-bridged and nonbridged structures are very close in energy with a low interconversion barrier of about 6.3 kcal/mol using highly correlated electronic calculations. For $B_2H_3^-$, Bigot et al.[9] have predicted that the nonbridged isomer H_2BBH^- is 8.3 kcal/mol lower in energy than the single-H-bridged structure $HB(H)BH^-$ at the HF/4-31G level. On the contrary, recent studies by Krempp et al.[3] and by Lammertsma and Ohwada[10] have found that $HB(H)BH^-$ is 6.6 and 7.8 kcal/mol lower in energy than H_2BBH^- at the MP2/6-31++G(d,p)//6-31++G(d,p) and MP2(full)/6-311G(d,p) levels, respectively.

Among these reactions of boron hydride anions, the reactions with CO_2, COS, and CS_2 are of particular interest since the three neutral species are isovalently analogous and are often used in mechanistic studies. Experimentally, the $B_2H_3^-$ anion undergoes interesting reactions[3] with CO_2, OCS, and CS_2 through similar reaction schemes as follows:

$$B_2H_3^- + CO_2 \rightarrow [B_2H_3O]^- + CO\ (77\%) \quad (1a)$$

$$\rightarrow [BH_2CO]^- + HBO\ (19\%) \quad (1b)$$

$$\rightarrow [BH_3CO] + BO^-\ (4\%) \quad (1c)$$

$$B_2H_3^- + OCS \rightarrow [B_2H_3S]^- + CO\ (85\%) \quad (2a)$$

$$\rightarrow [BH_2CO]^- + HBS\ (10\%) \quad (2b)$$

$$\rightarrow [B_2H_3O]^- + CS\ (5\%) \quad (2c)$$

$$B_2H_3^- + CS_2 \rightarrow [B_2H_3S]^- + CS\ (100\%) \quad (3)$$

The major products $[B_2H_3O]^-$ or $[B_2H_3S]^-$ are presumably formed by oxygen or sulfur extraction, respectively, while another abundant and unusual product $[BH_2CO]^-$ is presumably formed by nucleophilic attack of $B_2H_3^-$ at the carbon of CO_2 and OCS. It is also shown that sulfur abstraction dominates over oxygen abstraction by a large factor in the reaction with OCS (eq 2a versus eq 2c). Similar sulfur-abstraction reaction is also found[3] between $B_3H_6^-$ and CS_2.

10.1021/jp002122j CCC: $19.00
Published on Web 11/30/2000

To our best knowledge, no theoretical study has been reported on the reactions of boron hydride anions. In order to gain some insight into the reaction mechanism of boron hydride anions, we choose the reaction $B_2H_3^- + CO_2$ as a representative system and analyze the detailed potential energy surface of this typical ion−molecule reaction. In this paper, the potential energy surface of the reaction $B_2H_3^- + CO_2$ is investigated at the B3LYP/6-311++G(d,p) and single-point CCSD(T)/6-311++G-(d,p) levels of theory. Based on the calculated results, the detailed mechanism for this reaction is suggested. Our calculated results are in good agreement with the experimental results by Krempp et al.[3] for the gas-phase reaction $B_2H_3^- + CO_2$, and may be helpful for understanding the chemistry of boron hydride anions.

2. Computational Methods

All calculations are performed using the Gaussian 98 program package.[11] Full geometry optimization are carried out at the B3LYP/6-311++G(d,p)[12] level of theory along with analytic vibrational frequency calculations in order to characterize the obtained structures as minima or as transition states (**TS**) on the potential energy surface. Atomic charges and bond orders are calculated using the natural population analysis (NPA) and natural bond orbital (NBO) methods[13] in order to gain some information about the charge distribution and the bonding character of various structures. The intrinsic reaction coordinate (IRC)[14] calculations are carried out at the B3LYP level for connecting the transition states to reactants and products. The single-point CCSD(T)/6-311++G(d,p)[15] calculations are also carried out in order to gain more reliable energetics. Unless otherwise specified, the final CCSD(T) relative energies (in kcal/mol) including the B3LYP zero-point vibration energies are used in the following discussions, by taking the reactant $HB(H)BH^- + CO_2$ as zero for reference.

3. Results and Discussion

The B3LYP geometries and NPA atomic charges of the reactant $B_2H_3^- + CO_2$ and five low-lying dissociation products are shown in Figure 1, and those of 12 $[B_2H_3CO_2]^-$ intermediates and 17 transition states are shown in Figure 2 and Figure 3, respectively. Note that the transition states connecting the isomer **c** and the product **A**, and isomer **a** and **c** are denoted as **TScA** and **TSac**, respectively, other transition states are also named in the same way. The total, relative, and zero-point vibration energies of the reactant, possible products, intermediate isomers, and transition states calculated by the B3LYP and CCSD(T) methods are listed in Table 1. Then, based on the CCSD(T) relative energies, an overall energetic profile of the potential energy surface (PES) for the reaction $B_2H_3^- + CO_2$ is given in Figure 4.

It is easily seen from Table 1 that the B3LYP relative energies are very close to the CCSD(T) values within 4 kcal/mol for most structures. The largest discrepancies lie in two dissociation products **A** and **B** which are 8.5 and 8.7 kcal/mol, respectively. As shown in Figure 4, we can easily see that the micro-processes of the reaction $B_2H_3^- + CO_2$ are very complex. Starting from the energy-rich reactant $B_2H_3^- + CO_2$, various low-lying intermediate isomers may be reached via low-lying transition states and finally dissociated into five low-lying dissociation products. The calculated results in this paper are organized as follows. Using the B3LYP geometries and the more reliable CCSD(T) energies, we will discuss the reactants and possible dissociation products, intermediate isomers, and transition states in sections 3.1, 3.2, and 3.3, respectively. The reaction channels

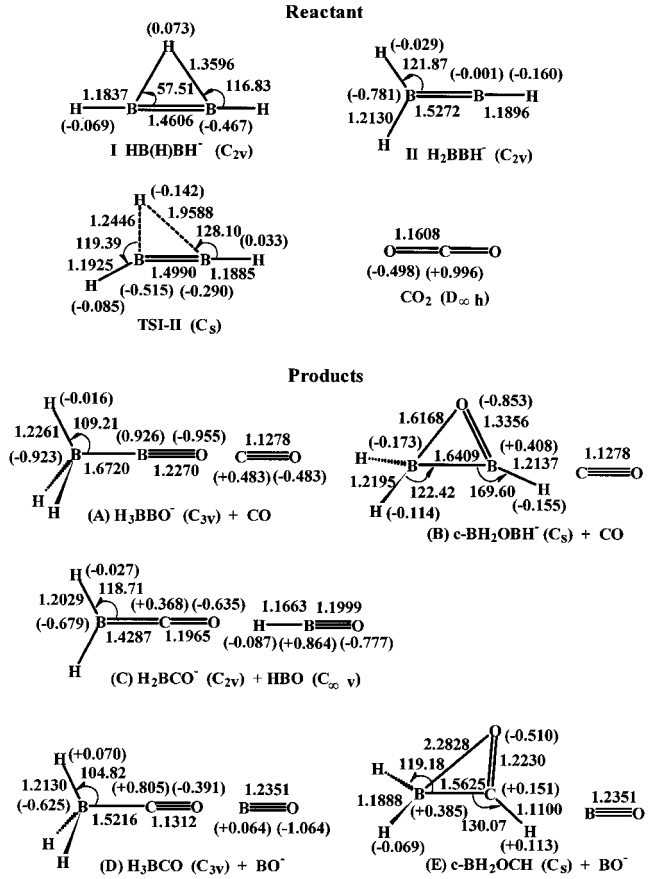

Figure 1. Geometries and NPA atomic charges of the reactant and five low-lying products calculated at the B3LYP/6-311++G(d,p) level. Bond lengths are in angstroms and bond angles in degrees.

leading to five low-lying dissociation products will discussed in section 3.4. Then, the overall mechanism for the reaction $B_2H_3^- + CO_2$ and a comparison with the SIFT experiments will be given in section 3.5.

3.1. Reactants and Possible Dissociation Products. In order to interpret the reactions of $B_2H_3^-$, it is important to gain the reliable energetics of this interesting anion system. As shown in Figure 1, the $B_2H_3^-$ anion may exist as two C_{2v} symmetry low-lying forms, i.e., the single-H-bridged isomer $HB(H)BH^-$ (**I**) and the nonbridged isomer H_2BBH^- (**II**). The B−B double bond length of **II** is 1.5272 Å, while the B−B distance of **I** is 0.0666 Å shorter due to the additional B−H−B three-center−two-electron (3c−2e) bridge bonding. The transition state between **I** and **II**, **TSI**−**II**, is also found at the B−B distance of 1.4990 Å. It is easily seen from Table 1 that the single-H-bridged isomer **I** lies 4.9 kcal/mol lower in energy than the nonbridged isomer **II** at the CCSD(T) level. Bigot et al.[9] have predicted that isomer **II** is 8.3 kcal/mol lower in energy than isomer **I** at the HF/4-31G level. On the contrary, recent studies by Krempp et al.[3] and by Lammertsma and Ohwada[10] have shown that **I** is 6.6 and 7.8 kcal/mol lower in energy than **II** at the higher MP2/6-31++G(d,p)//HF/6-31++G(d,p) and MP2-(full)/6-311G(d,p) levels, respectively. Our CCSD(T) results are in agreement with the recent MP2//HF[3] and MP2[10] calculations. It should be pointed out that the double-H-bridged isomer of its neutral isoelectronic partner B_2H_4 is also favored when highly electron correlation is included.[6] On the other hand, the respective **II** → **I** and **I** → **II** isomerization barriers are 0.2 and 4.9 kcal/mol at the CCSD(T) level. The very low **II** → **I** barrier indicates that the nonbridged isomer **II** is kinetically rather unstable and only the stable bridged isomer **I** may exist under

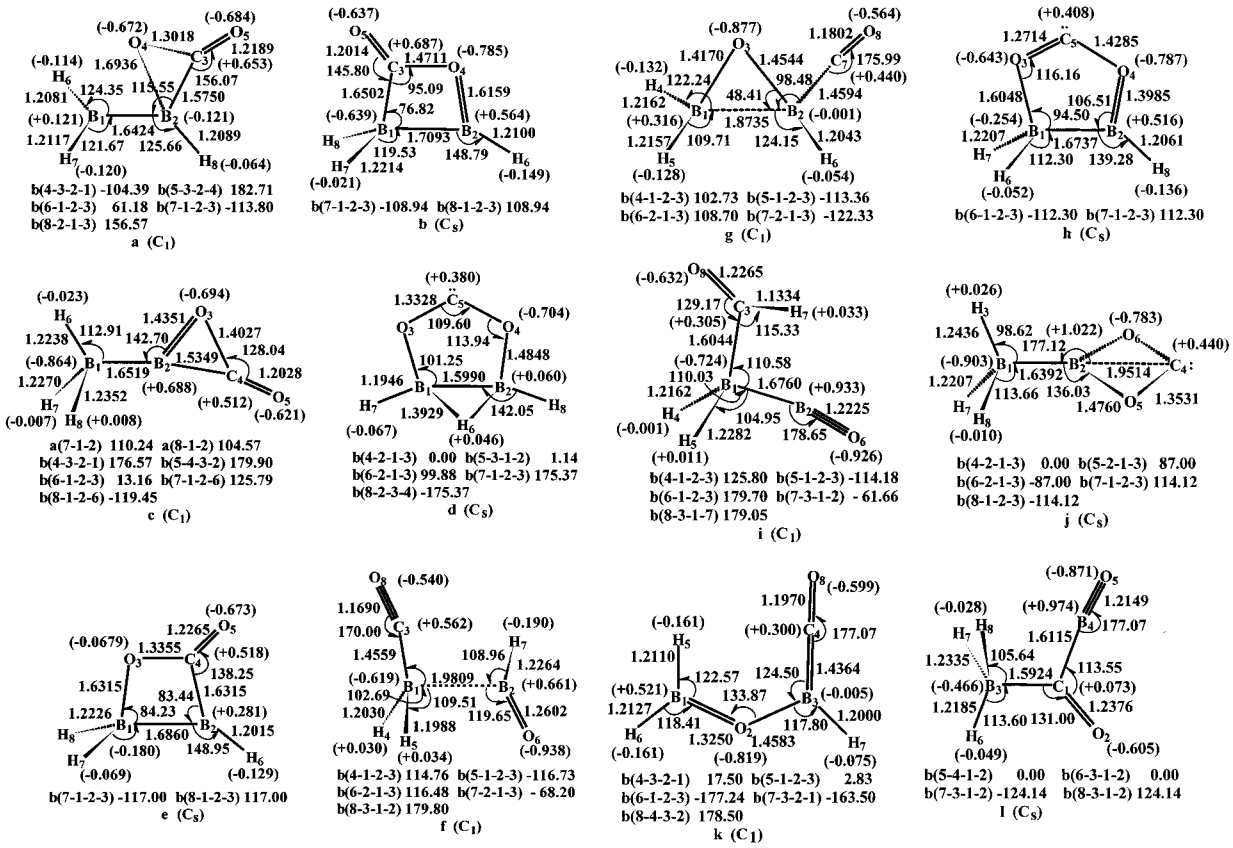

Figure 2. Geometries and NPA atomic charges of the 12 $[B_2H_3CO_2]^-$ intermediate isomers calculated at the B3LYP/6-311++G(d,p) level. Bond lengths are in angstroms and bond angles in degrees.

the thermal conditions in the SIFT experiments.[3] In the following discussions, we only take **(R)** $HB(H)BH^- + CO_2$ as the initial reactant.

Experimentally, three dissociation products $[B_2H_3O]^- + CO$ (77%), $[BH_2CO]^- + HBO$ (19%), and $[BH_3CO] + BO^-$ (4%) have been found[3] in the reaction $B_2H_3^- + CO_2$ under thermal conditions. It is interesting to note that $[B_2H_3O]^-$ and $[BH_2CO]^-$ are isoelectronic with $[BH_3CO]$, and BO^- is isoelectronic with CO. As shown in Figure 1, both $[B_2H_3O]^-$ and $[BH_3CO]$ may exist as two low-lying isomers. The electronic structures of the linear H_3BBO^-, cyclic c-BH_2OBH^-, and BO^- anions are very similar to those of the neutral linear H_3BCO, c-BH_2OCH, and CO, respectively. As shown in Table 1, the CCSD(T) relative energies of the five low-lying products may be given in parentheses as follows: **(A)** $H_3BBO^- + CO$ (−84.5), **(B)** c-$BH_2OBH^- + CO$ (−42.1), **(C)** $H_2BCO^- + HBO$ (−39.0), **(D)** $H_3BCO + BO^-$ (−39.9), and **(E)** c-$BH_2OCH + BO^-$ (−13.2). Since hydride transfer to CO_2 is very common in gas-phase reaction of anions, and loss of BH_3 has also been found in reactions of $B_3H_6^-$ anion with acrolein and acrylonitrile,[3] two other products $HCO_2^- + B_2H_2$ and $BCO_2^- + BH_3$ are also considered. Several products calculated preliminarily in this paper such as **(F)** $HCO^- + H_2BBO$, **(G)** c-BOC═$O^- + BH_3$, **(H)** $HCO_2^- + B_2H_2$, **(I)** $H_2BO^- + HBCO$ are shown to be 14.1, 27.8, 58.1, and 23.4 kcal/mol higher than the initial reactant **(R)** $HB(H)BH^- + CO_2$ in energy, respectively. Under thermal conditions where any significant barriers above the reactants will be insurmountable, the formation of the high-lying products **F**, **G**, **H,** and **I** cannot compete with those of the five low-lying products **A**, **B**, **C**, **D,** and **E** thermodynamically in the reaction $HB(H)BH^- + CO_2$. Actually, no products **F**, **G**, **H,** and **I** are detected in the SIFT experiments.[3] Thus, the formation of the products **F**, **G**, **H,** and **I** will not be considered further.

3.2. $[B_2H_3CO_2]^-$ Intermediate Isomers. According to the geometrical features shown in Figure 2, the 12 intermediate isomers may be classified into four groups, i.e., three-membered rings (**a**, **c**, and **g**), four-membered rings (**b**, **e**, and **j**), five-membered rings (**d** and **h**), and open isomers (**f**, **i**, **k**, and **l**). The NPA atomic charges of these isomers are also given in Figure 2. It is likely that there is a minimum structure of isomer **f** with a different O−B−B−C dihedral angle and a transition state of isomerization of HBO part between them. However, such minimum structure and transition state cannot be found at the B3LYP/6-311++G(d,p) level of theory in spite of some efforts. Also, we cannot find a minimum structure of isomer **i** with a different O−C−B−B dihedral angle in our calculations.

It is interesting to discuss the B−B bond lengths in various isomers since they change remarkably. The B−B distances in isomers **a**, **c**, and **j** are 1.6424, 1.6519, and 1.6392 Å, respectively, which are very close to the value 1.64 Å of normal B−B single bond. The B−B distances in the cyclic **b**, **e**, and **h** are slightly longer by 0.07, 0.05, and 0.03 Å than the value 1.64 Å, respectively, which may be due to the ring-strain in these isomers. On the contrary, the B−B distance in cyclic isomer **d** is shortened by 0.04 Å due to the additional B−H−B 3c−2e bonding. The B−B single bond in the open isomer **i** is slightly elongated by 0.04 Å compared to the normal B−B single bond. A very long B−B distance of 1.9808 Å is found in isomer **f**, which suggests a loose bonding between the HBO and H_2BCO^- fragments. For the three-membered ring **g**, a long B−B distance of 1.8735 Å is also found, it may easily ring-open to the linear isomer **k**.

As shown in Table 1, all 12 intermediate isomers considered in this paper lie energetically below the reactant **(R)** $HB(H)BH^- + CO_2$. The CCSD(T) relative energies (in kcal/mol) may be listed (in parentheses) according to the thermodynamical stability

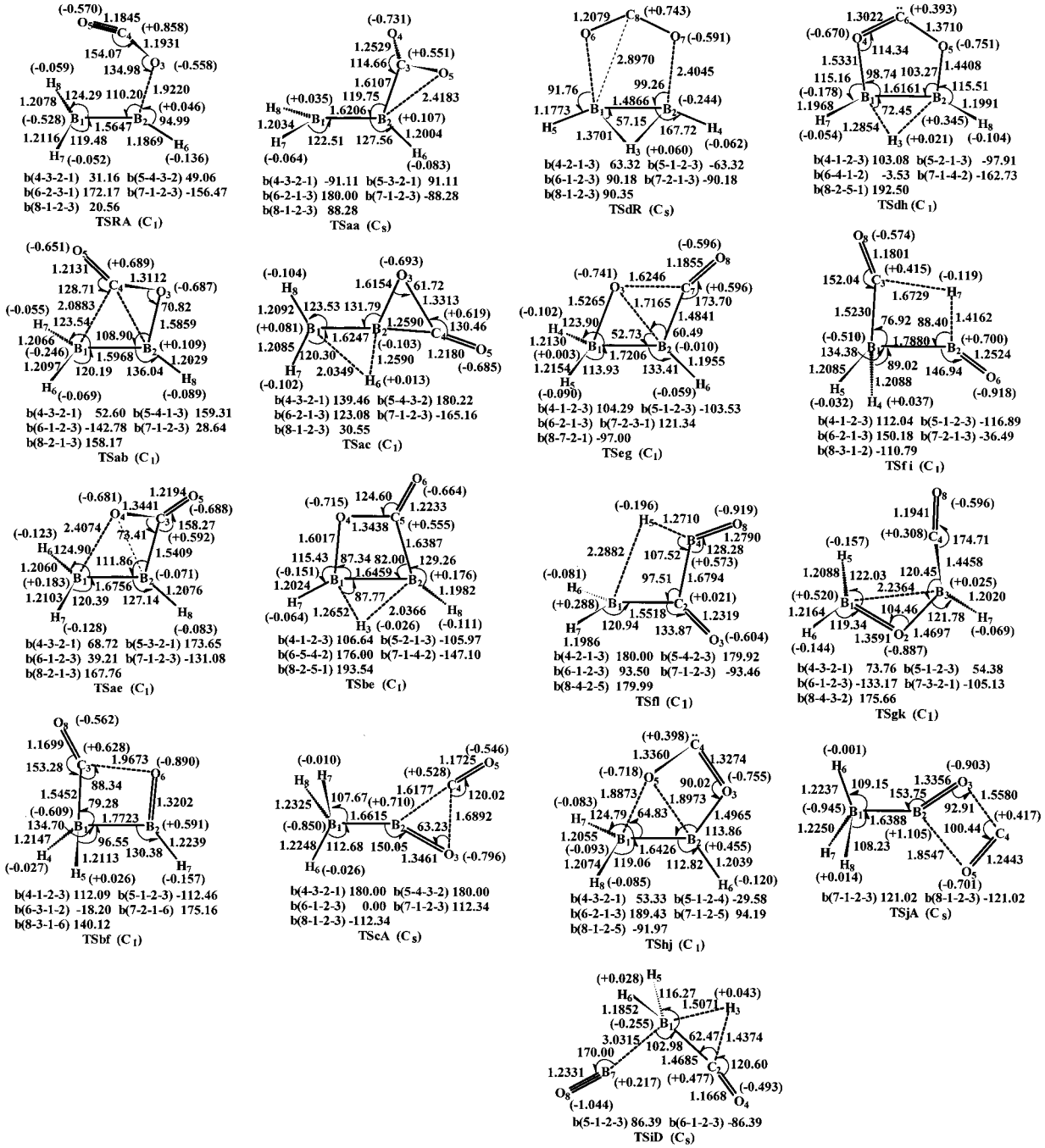

Figure 3. Geometries and NPA atomic charges of the 17 transition states calculated at the B3LYP/6-311++G(d,p) level. Bond lengths are in angstroms and bond angles in degrees.

as follows: **i** (−88.9) < **l** (−74.2) < **f** (−60.5) < **b** (−58.0) < **g** (−55.9) < **k** (−55.2) < **h** (−43.4) < **c** (−43.2) < **d** (−39.8) < **e** (−34.5) < **a** (−33.7) < **j** (−33.5). It should be noted that isomer **g** lies very close to isomer **k** and isomer **a** lies very close to isomers **e** and **j** in energy within 1 kcal/mol.

3.3. Transition States and Isomerization. To make clear the connection between the isomers and dissociation products, 17 transition states are obtained as shown in Figure 3 and Table 1 and their relation with reactants and products are confirmed by the IRC calculations. Note that the degenerate transition state **TSaa** is related to the oxygen exchange within isomer **a**, the transition states **TScA**, **TSdR**, **TSjA**, and **TSiD** to the respective dissociation of isomers **c**, **d**, **j**, and **i**, and other transition states to the isomerization between various isomers. The CCSD(T) relative energies (in kcal/mol) of these transition states are shown as follows: **TSRA** (+16.6), **TSaa** (−22.8), **TSab** (−32.5), **TSac** (−30.6), **TSae** (−27.3), **TSbe** (−32.8), **TSbf** (−50.4), **TScA** (−42.1), **TSdR** (+15.2), **TSdh** (−39.4), **TSeg** (−32.4), **TSfi** (−43.9), **TSfl** (−35.9), **TSgk** (−50.9), **TShj** (−13.8), **TSjA** (−26.3), and **TSiD** (−22.2). We can easily see that all these transition states are energetically below the reactant **(R)** except for **TSRA** and **TSdR**. By means of the energies of the intermediate isomers, dissociation fragments, and transition states, we can discuss the kinetical stability of 12 intermediate isomers.

First, we consider the kinetical stability of the three three-membered rings **a**, **c**, and **g**. The **a** → **b**, **a** → **c**, and **a** → **e** isomerization barriers via **TSab**, **TSac**, and **TSae** are 1.2, 3.1, and 6.4 kcal/mol, respectively. No transition state is found for the dissociation of isomer **a** into **(R)** $HB(H)BH^-$ + CO_2 and

TABLE 1: Total Energies (*E*, in au), Zero-Point Vibrational Energies (ZPVE, in au), and Relative Energies (RE, in kcal/mol) of the Reactant, Possible Products, Intermediate Isomers, and Transition States Calculated at the B3LYP/6-311++G(d,p) and Single-point CCSD(T)/6-311+G(d,p) Levels

	B3LYP			CCSD(T)	
methods species	*E*	ZPVE	RE	*E*	RE
HB(H)BH$^-$ (**I**)	(−51.463 504)	(0.027 914)	(0.0)	(−51.268 882)	(0.0)
H_2BBH^- (**II**)	(−51.458 297)	(0.027 367)	(+2.9)	(−51.260 951)	(+4.7)
TSI−II	(−51.456 409)	(0.026 525)	(+3.6)	(−51.259 641)	(+4.9)
(R) HB(H)BH$^-$ + CO_2	−240.110 419	0.039 599	0.0	−239.490 141	0.0
(A) H_3BBO^- + CO	−240.231 145	0.039 251	−76.0	−239.624 534	−84.5
(B) c-BH_2OBH^- + CO	−240.163 581	0.039 593	−33.4	−239.556 939	−42.1
(C) H_2BCO^- + HBO	−240.176 443	0.039 919	−41.2	−239.552 581	−39.0
(D) H_3BCO + BO^-	−240.169 256	0.040 409	−36.4	−239.554 600	−39.9
(E) c-BH_2OCH + BO^-	−240.129 737	0.041 545	−10.9	−239.513 051	−13.2
(F) HCO^- + H_2BBO	−240.086 650	0.036 318	+12.9	−239.464 387	+14.1
(G) c-BOC=O^- + BH_3	−240.060 349	0.038 231	+30.6	−239.444 339	+27.8
(H) HCO_2- + B_2H_2	−240.025 339	0.041 215	+54.4	−239.399 067	+58.1
(I) H_2BO^- + HBCO	−240.070 705	0.033 696	+21.2	−239.447 022	+23.4
a	−240.169 418	0.043 329	−34.7	−239.547 543	−33.7
b	−240.202 676	0.044 250	−55.0	−239.587 251	−58.0
c	−240.180 588	0.041 986	−42.5	−239.561 453	−43.2
d	−240.172 480	0.045 405	−35.3	−239.559 375	−39.8
e	−240.167 954	0.044 010	−33.3	−239.549 509	−34.5
f	−240.211 585	0.042 637	−61.6	−239.589 521	−60.5
g	−240.203 919	0.044 095	−55.9	−239.584 002	−55.9
h	−240.177 668	0.044 553	−39.1	−239.564 287	−43.4
i	−240.254 838	0.045 505	−86.9	−239.637 740	−88.9
j	−240.156 880	0.041 124	−28.2	−239.545 116	−33.5
k	−240.206 836	0.043 930	−57.8	−239.582 381	−55.2
l	−240.230 628	0.0431 74	−73.2	−239.611 918	−74.2
TSRA	−240.091 766	0.0402 35	+12.1	−239.464 277	+16.6
TSaa	−240.158 819	0.0421 46	−28.8	−239.528 953	−22.8
TSab	−240.163 422	0.0436 01	−30.7	−239.545 914	−32.5
TSac	−240.164 092	0.0419 31	−32.2	−239.541 362	−30.6
TSae	−240.156 222	0.0428 86	−26.7	−239.536 992	−27.3
TSbe	−240.164 707	0.0432 08	−31.8	−239.546 036	−32.8
TSbf	−240.193 545	0.0428 22	−50.1	−239.573 723	−50.4
TScA	−240.175 399	0.0404 33	−40.3	−239.558 051	−42.1
TSdR	−240.090 647	0.0404 19	+12.9	−239.466 688	+15.2
TSdh	−240.170 797	0.0440 84	−35.1	−239.557 440	−39.4
TSeg	−240.162 595	0.0435 84	−30.2	−239.545 796	−32.4
TSfi	−240.183 551	0.0410 85	−45.0	−239.561 610	−43.9
TSfo	−240.170 597	0.0409 57	−36.9	−239.548 656	−35.9
TSgk	−240.187 392	0.0432 84	−52.3	−239.574 847	−50.9
TShj	−240.127 227	0.0429 52	−8.4	−239.515 538	−13.8
TSjA	−240.145 599	0.039 596	−22.1	−239.532 074	−26.3
TSiD	−240.144 621	0.039 285	−21.7	−239.525 179	−22.2

H_2BBH^- + CO_2, and the respective dissociation energies are 33.7 and 38.4 kcal/mol. Considering the energetics, the **a** → **b** conversion via **TSab** is the most possible conversion for isomer **a**. For isomer **c**, the **c** → **a**, **c** → **A** conversion barrier via **TSac** and **TScA** are 12.6 and 1.1 kcal/mol, respectively. No transition state is found for the **c** → **G** dissociation process and the corresponding dissociation energy is 71.0 kcal/mol. It seems that the **c** → **A** conversion via **TScA** is the most possible conversion for isomer **c**. For isomer **g**, the respective **g** → **e** and **g** → **k** isomerization barriers via **TSeg** and **TSgk** are 23.5 and 5.0 kcal/mol. No transition state is found for the **g** → **B** dissociation process and the corresponding dissociation energy is 13.8 kcal/mol. It is shown that the barriers of 1.2, 1.1, and 5.0 kcal/mol stabilize isomers **a**, **c**, and **g**, respectively.

Second, we consider the three four-membered rings **b**, **e**, and **j**. For isomer **b**, the **b** → **a**, **b** → **e,** and **b** → **f** isomerization barriers via **TSab**, **TSbe**, and **TSbf** are 25.5, 25.2, and 7.6 kcal/mol, respectively. For isomer **e**, the respective **e** → **a**, **e** → **b,** and **e** → **g** isomerization barriers via **TSae**, **TSbe**, and **TSeg** are 7.2, 1.7, and 2.1 kcal/mol. For isomer **j**, the **j** → **h,** and **j** → **A** conversion barriers via **TShj** and **TSjA** are 19.7 and 11.3 kcal/mol, respectively. It is shown that the lowest conversion barriers for isomers **b**, **e**, and **j** are 7.6, 1.7, and 11.3 kcal/mol, respectively.

Third, we discuss the two five-membered rings **d** and **h**. Isomers **d** and **h** may easily isomerize to each other via **TSdh** and the respective **d** → **h** and **h** → **d** isomerization barriers are 0.4 and 4.0 kcal/mol. On the other hand, the **d** → **R** and **h** → **j** conversion barriers via **TSdR** and **TShj** are 55.0 and 29.6 kcal/mol, respectively. It is shown that the respective low barriers of 0.4 and 4.0 kcal/mol stabilize isomer **d** and isomer **h**.

Finally, we consider the four open isomers **f**, **i**, **k**, and **l**. For isomer **f**, the **f** → **b**, **f** → **i,** and **f** → **l** isomerization barriers via **TSbf**, **TSfi**, and **TSfl** are 10.1 16.1, and 24.6 kcal/mol, respectively. No transition state is found for the breaking of the long B−B bond of isomer **f**, the dissociation energy of **f** into **C** is 21.5 kcal/mol. For the most low-lying isomer **i**, the respective **i** → **f**, and **i** → **D** conversion barriers via **TSfi** and **TSiD** are 45.0 and 66.7 kcal/mol. No transition state is found for the breaking of the B−B or B−C single bonds of isomer **i**, and the **i** → **E** and **i** → **F** dissociation energies are 78.0 and 101.8 kcal/mol, respectively. For isomers **k** and **l**, the **k** → **g** isomerization barrier via **TSgk** and the **l** → **f** isomerization

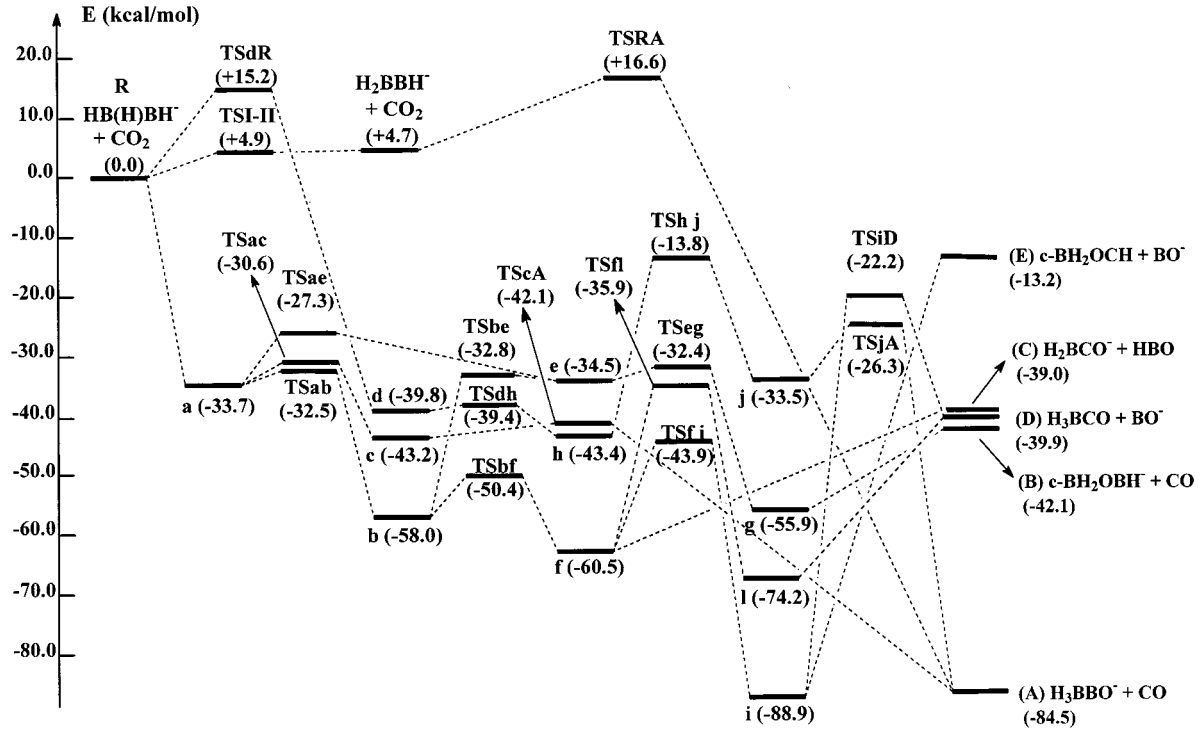

Figure 4. Schematic profile of the potential energy surface of the reactions of $B_2H_3^- + CO_2$ calculated at the CCSD(T)/6-311++G(d,p)//B3LYP/6-311++G(d,p) level including the B3LYP zero-point vibrational energies.

barrier via **TSfl** are 4.3 and 38.3 kcal/mol, respectively. No transition state is found for the **k** → **I** and **l** → **D** dissociation processes and the respective **k** → **I** and **l** → **D** dissociation energies are 78.6 and 34.3 kcal/mol. Thus, the respective barriers of 10.1, 45.0, 4.3, and 34.3 kcal/mol stabilize isomers **f**, **i**, **k**, and **l**.

From the discussions above, the kinetical stability (in kcal/mol) of the 12 isomers may be listed (in parentheses) as follows: **i** (45.0) > **l** (34.3) > **j** (11.3) > **f** (10.1) > **b** (7.6) > **g** (5.0) > **k** (4.3) > **h** (4.0) > **e** (1.7) > **a** (1.2) > **c** (1.1) > **d** (0.4). It is clear that isomers **a**, **c**, **d**, and **e** are kinetically rather unstable.

3.4. Formation of Dissociation Products. From the PES for the reaction $HB(H)BH^- + CO_2$ presented in Figure 4, we know that starting from the reactant **(R)** $HB(H)BH^- + CO_2$, many low-lying intermediate isomers may be reached and finally dissociate into five low-lying products **(A)** H_3BBO^- + CO, **(B)** c-BH_2OBH^- + CO, **(C)** H_2BCO^- + HBO, **(D)** $H_3BCO + BO^-$, and **(E)** c-$BH_2OCH + BO^-$. Note that the products **A** and **B**, **C**, and **D** and **E** are the respective low-lying isomeric forms of the observed[3] products $[B_2H_3O]^-$ + CO, $[BH_2CO]^-$ + HBO, and $[H_3BCO]$ + BO^-. We now discuss the details of the formation of these five low-lying products.

3.4.1. Formation of (A) H_3BBO^- + CO and (B) c-BH_2OBH^- + CO. The formation of products **A** and **B** is actually associated with the oxygen abstraction of $HB(H)BH^-$ from CO_2. Two ways of attack of $HB(H)BH^-$ toward CO_2, i.e., oxygen attack and carbon attack, are considered in this paper. From the PES presented in Figure 4, we can obtain three possible pathways for product **A** and two for product **B** as follows.

path A1: **R → TSI−II → H_2BBH^- + CO_2 → TSRA → A**

path A2: **R → TSdR → d → TSdh → h → TShj → j → TSjA → A**

path A3: **R → a → TSac → c → TScA → A**

path B1: **R → a → TSab → b → TSbe → e → TSeg → g → B**

path B2: **R → a → TSae → e → TSeg → g → B**

Two oxygen-attack pathways are given in path A1 and path A2. As shown in path A1, $HB(H)BH^-$ may isomerize to the open isomer H_2BBH^-, followed by the oxygen-abstraction from CO_2 to form the final product **A**. On the other hand, as shown in path A2, $HB(H)BH^-$ may ring addition with CO_2 to form the five-membered ring intermediate **d**, which may take subsequent low-lying pathway to the final product **A**. However, both path A1 and path A2 are prevented by the activation barriers of 16.6 and 15.2 kcal/mol above the reactant **R** at the oxygen-abstraction and the ring-addition steps, respectively. Thus, both oxygen-attack pathways are energetically unfeasible under thermal conditions.

The carbon-attack of $HB(H)BH^-$ toward CO_2 may lead to the three-membered ring intermediate **a** with no barrier. Once isomer **a** is formed, it may isomerize to three isomers **c**, **b**, and **e** via **TSac**, **TSab**, and **TSae** with the respective **a** → **c**, **a** → **b**, and **a** → **e** conversion barriers to be 3.1, 1.2, and 6.4 kcal/mol. As shown in path A3, isomer **c** may dissociate into product **A** via **TScA** and the **c** → **A** conversion barrier is only 1.1 kcal/mol. As shown in path B2, isomer **e** may also isomerize to **g** and then dissociate directly into product **B**, the respective **e** → **g** isomerization barrier and **g** → **B** dissociation energy are 2.1 and 13.8 kcal/mol. The **b** → **e** conversion provides another pathway leading isomer **a** to **e** as shown in path B1, the **b** → **e** isomerization barrier is 25.2 kcal/mol. All the transition states and intermediates involved in path A3, path B1 and path B2 are energetically lower than the reactant **R**; thus, in principle all these pathways may contribute more or less to the formation of the products **A** and **B**. Considering that from the common intermediate **a** the **a** → **c** isomerization barrier is 3.3 kcal/mol lower than that of **a** → **e** conversion and product **A** is 42.4 kcal/

mol lower than product **B** in energy, path A3 is energetically more competitive than path B2. Notice that the intermediate **b** may lead mainly to isomer **f** other than isomer **e** involved in path B1 because the **b** → **f** isomerization barrier is 17.6 kcal/mol lower than that for **b** → **e** conversion, and the **a** → **c** isomerization barrier is very close (1.9 kcal/mol higher at the CCSD(T) level but 1.5 kcal/mol lower at the B3LYP level) to that for **a** → **b** conversion in energy, it seem that path A3 is more competitive than path B1. From the discussion above, we conclude that the formation of product **A** is more favorable than that of product **B**.

3.4.2. Formation of (C) H_2BCO^- + HBO. The isomer **f** may be the most likely precursor for the formation of product **C** considering the loose-bound H_2BCO^- and HBO parts in isomer **f**. From Figure 4, we can obtain two low-lying pathways for the formation of product **C** as follows.

path C1: **R → a → TSab → b → TSbf → f → C**

path C2: **R → a → TSae → e → TSbe → b → TSbf → f → C**

We can also see that all transition states and intermediates involved in path C1 and path C2 are energetically lower than the reactant **R**, thus both pathways are energetically feasible for the formation of product **C**. The only difference between path C1 and path C2 is that an additional intermediate **e** is involved between isomers **a** and **b** in path C2. As shown in path C1, once the intermediate **a** is formed from the reactant **R**, it may take the subsequent isomerization of **a** → **b** and **b** → **f** over the respective isomerization barriers of 1.2 and 7.6 kcal/mol. No transition state is found for the dissociation of **f** into product **C** and the dissociation energy is 21.5 kcal/mol. Since the **a** → **e** conversion barrier in path C2 is 5.2 kcal/mol higher than that for **a** → **b** in path C1, it seems that path C2 is less important than path C1 for the formation of product **C**.

3.4.3. Formation of (D) H_3BCO + BO^- and (E) c-BH_2OCH + BO^-. From the PES presented in Figure 4, we can obtain four low-lying pathways for product **D** and two for product **E** as follows.

path D1: **R → a → TSab → b → TSbf → f → TSfi → i → TSiD → D**

path D2: **R → a → TSae → e → TSbe → b → TSbf → f → TSfi → i → TSiD → D**

path D3: **R → a → TSab → b → TSbf → f → TSfl → l → D**

path D4: **R → a → TSae → e → TSbe → b → TSbf → f → TSfl → l → D**

path E1: **R → a → TSab → b → TSbf → f → TSfi → i → E**

path E2: **R → a → TSae → e → TSbe → b → TSbf → f → TSfi → i → E**

It can be easily seen that all transition states and intermediates involved in these six pathways are lower in energy than the reactant **R**; thus both products **D** and **E** may be produced. It seems that path D1, path D3, and path E1 are more competitive than path D2, path D4, and path E2, respectively, since the **a** → **e** isomerization barrier is 5.2 kcal/mol higher than that for **a** → **b**. Notice that a common intermediate **f** is involved in all the six pathways, and the low-lying pathways leading the reactant **R** to isomer **f** have already been discussed in section 3.4.2. Once isomer **f** is formed, it may isomerize to the intermediates **i** via **TSfi** and subsequently dissociate into product **D** via **TSiD** as shown in path D1 and path D2, or into product **E** directly as shown in path E1 and path E2. The respective **f** → **i** and **i** → **D** conversion barriers and the **i** → **E** dissociation energy are 16.6, 66.7, and 75.7 kcal/mol. Since the **i** → **D** conversion barrier is 9.0 kcal/mol lower than the **i** → **E** dissociation energy and product **D** is 26.7 kcal/mol lower than product **E** in energy, it seems that path D1 and path D2 are more competitive than path E1 and path E2, respectively. Moreover, isomer **f** may isomerize to the intermediates **l** via **TSfl** and subsequently dissociate directly into product **D** as shown in path D3 and path D4. The respective **f** → **l** conversion barrier and **l** → **D** dissociation energy are 24.6 and 34.3 kcal/mol. Since the **f** → **l** conversion barrier is 10.2 lower than that for **i** → **D** in energy, it seems that path D3 and path D4 are more competitive than path D1 and path D2, respectively. From the discussion above, we conclude that the formation of product **D** is more favorable than that of product **E**.

3.5. Reaction Mechanism and Comparison with Experiments. As discussed in section 3.1 that the nonbridged isomer H_2BBH^- is kinetically rather unstable with respect to isomerization into the stable bridged isomer $HB(H)BH^-$, we only discuss the reaction of $HB(H)BH^-$ with CO_2. The presentation of the atomic charges may be helpful for understanding the reaction mechanism of the interesting electron-deficient $HB(H)BH^-$ anion with CO_2. As shown in Figure 1, the NPA atomic charges of the boron atom of $HB(H)BH^-$ and the oxygen and carbon atoms of CO_2 are −0.467, −0.498, and +0.996 au, respectively. Two electrophilic oxygen-attack pathways of $HB(H)BH^-$ toward CO_2 are considered in this paper as shown in path A1 and path A2. However, the oxygen abstraction step in path A1 and the ring-addition step in path A2 are prevented by the respective barriers of 16.6 and 15.2 kcal/mol above the reactant **R** in energy. This may be due to the repulsion of the negative charges resided on the boron and oxygen atoms. On the other hand, the nucleophilic carbon attack of $HB(H)BH^-$ toward CO_2 may form the low-lying adduct **a** with no barrier, followed by subsequent isomerization and final dissociation leading to five low-lying products **A**, **B**, **C**, **D**, and **E** as shown in various low-lying pathways paths A3, B1, B2, D1, D2, D3, D4, E1, E2. The large energy released in the **R** → **a** association step may promote the subsequent isomerization and dissociation steps. From the discussion above, the mechanism for the reaction of $HB(H)BH^-$ + CO_2 may be referred to as the nucleophilic attack of $HB(H)BH^-$ toward CO_2, subsequent isomerization and final dissociation.

It is interesting that the nucleophilic reaction is favored for the electron-deficient $HB(H)BH^-$ anion toward CO_2 in contrast to the positive and neutral electron-deficient boron species such as BH_4^+ and BH_3, which may form various donor−acceptor complexes with CO_2, COS, and CS_2 by electrophilic attack.[16]

A further comparison of our calculated results with the available experimental results may also be useful. Experimentally, the dissociation products $B_2H_3O^-$ + CO (77%), BH_2CO^- + HBO (19%), and BH_3CO + BO^- (4%) have been detected[3] for the gas-phase reaction of $B_2H_3^-$ + CO_2 under thermal conditions. In our calculations, the nonbridged isomer H_2BBH^- is kinetically rather unstable with respect to isomerization to the bridged isomer $HB(H)BH^-$. The preliminary calculations for the possible products **F**, **G**, **H,** and **I** show that they are 14.1, 27.8, 58.1, and 23.4 kcal/mol higher than the initial reactant **R**, respectively, and thus will not be produced in the reaction

TABLE 2: Calculated Entropy *S* (in cal mol^{-1} K^{-1}) Values of the Isomers and Transition States at the B3LYP/6-311++G(d,p) Level

species	*S*	species	*S*	species	*S*
a	73.043	**j**	75.294	**TSdR**	75.150
b	72.596	**k**	74.507	**TSdh**	66.338
c	76.024	**l**	75.571	**TSeg**	68.854
d	66.770	**TSab**	69.220	**TSfi**	72.012
e	71.627	**TSac**	70.627	**TSfl**	75.605
f	77.650	**TSae**	71.031	**TShj**	68.881
g	72.767	**TSbe**	69.035	**TSjA**	76.487
h	68.647	**TSbf**	70.039	**TSiD**	84.932
i	75.051	**TScA**	75.037		

of $HB(H)BH^-$ with CO_2. As discussed in section 3.4, five low-lying products **A**, **B**, **C**, **D,** and **E** are all energetically accessible in the reaction $HB(H)BH^- + CO_2$, among which products **A** and **B** are related to $B_2H_3O^- + CO$, product **C** to $BH_2CO^- +$ HBO, and products **D** and **E** to $BH_3CO + BO^-$. Thus our calculations can reasonably predict the formation of the observed products.

Moreover, it is interesting to discuss the possible product distribution of the reaction $HB(H)BH^-$ with CO_2 based on our calculated mechanism. Though the quantitative branching ratio for observed products must be determined by the detailed dynamics of the reaction, some qualitative conclusion may be drawn based on our calculations. As discussed in section 3.4, the formation of product **A** is more favorable than that of product B and the formation of product **D** is more favorable than that of product **E**. It seems that the products $B_2H_3O^- + CO$, $BH_2CO^- +$ HBO, and $BH_3CO + BO^-$ are produced mainly as the forms of **A**, **C**, and **D**, respectively. For simplicity, we only make comparisons between the most feasible pathways for the formation of products **A**, **C,** and **D** as follows.

path A3: **R → a → TSac → c → TScA → A**

path C1: **R → a → TSab → b → TSbf → f → C**

path D3: **R → a → TSab → b → TSbf → f → TSfl → l → D**

Since starting from the common intermediate, the **f → l** isomerization barrier and the subsequent **l → D** dissociation energy in path D3 are 3.1 and 12.8 kcal/mol higher in energy, respectively, than the **f → C** dissociation energy in path C1. It seems that the formation of product **D** is less favorable than that of product **C**. On the other hand, since starting from the common intermediate **a,** the **a → c** barriers in path A3 are very close (1.5 kcal/mol lower at the B3LYP level but 1.9 kcal/mol higher at the CCSD(T) level) to the **a → b** barriers in path C1, it seems that the formation of products **A** and **C** may compete with each other. From the discussion above, it may conclude that the main products in this reaction are **A** and **C** while the minor product is **D**, which is in good agreement with the experimental abundance of the products $B_2H_3O^- + CO$ (77%), $BH_2CO^- +$ HBO (19%), and $BH_3CO + BO^-$ (4%).

In the preceding discussions, we have made use of the calculated barrier heights to probe qualitatively the possible reaction mechanism of the title reaction. Actually, we might expect the prefactors *A* to play equally important roles in distinguishing between the reaction pathways, since the present system involves a variety of tight and loose transition state structures. Table 2 lists the calculated entropies *S* which is reflected in *A* factors, of the relevant isomers and transition states at the B3LYP/6-311++G(d,p) level. Fortunately, these *S* values do not vary widely from each other (around 70 cal mol^{-1} K^{-1}) except for **TSiD** (84.932 cal mol^{-1} K^{-1}). Therefore, the influence of the differences in *S* (ΔS) on the rate constants for various isomerization processes may be less significant compared to those of the barrier heights (ΔE). For simplicity, we take the processes **a → b**, **a → c**, and **a → e** as examples. The three processes are the first and rate-determining steps for the formation of the main products and their barriers vary within 5 kcal/mol. For the three processes, the $-\Delta E/RT$ values are -2.03, -5.24, and -10.64, while the $\Delta S/R$ values are -1.92, -1.22, and -1.01, respectively. Note that *T* is 298 K and *R* is a constant 8.314 J mol^{-1} K^{-1}. The negative ΔS values mean that the transition states **TSab**, **TSac**, and **TSae** are tight compared with isomer **a**. We can see that for the three processes, the influences of ΔS on the rate constants are just the opposite to those of ΔE. However, since the changes of $-\Delta E/RT$ values are much greater than those of $\Delta S/R$ values, the changes of $\exp(-\Delta E/RT)$ values are expected to be even greater than $\exp(\Delta S/R)$ values. This indicates that the barrier heights mainly determine the competition of the processes **a → b**, **a → c**, and **a → e** while the effects of prefactors *A* are relatively small. Certainly, the other processes with large barrier height changes are mainly governed by the barrier heights. Therefore, it is safe to discuss the mechanism of the complex title reaction by simply using barrier heights.

Very similar ion−molecule reactions of $B_2H_3^-$ with CS_2 and COS have also been found[3] by Krempp et al. It is also noticed that the $B_3H_6^-$ anion may extract sulfur atom from CS_2.[3] Our calculated potential energy surface of the gas-phase reaction $B_2H_3^- + CO_2$ may serve as a good model for understanding the reaction mechanisms of the electron-deficient boron hydride anions.

IV. Conclusions

The CCSD(T) calculations show that the H-bridged isomer of the diborane(3) anion, $HB(H)BH^-$ is thermodynamically 4.7 kcal/mol more stable than the nonbridged isomer H_2BBH^-, which is kinetically rather unstable. The detailed potential energy surface of the reaction $B_2H_3^- + CO_2$ is investigated at the B3LYP and CCSD(T) levels of theory. The thermodynamical and kinetical stability of intermediate isomers are determined. The possible reaction pathways are probed and five low-lying products **(A)** $H_3BBO^- + CO$, **(B)** $c\text{-}BH_2OBH^- + CO$, **(C)** $H_2BCO^- +$ HBO, **(D)** $H_3BCO + BO^-$, and **(E)** $c\text{-}BH_2OCH + BO^-$ are shown to be both thermodynamically and kinetically accessible thus may be observed by experiments. Our calculated mechanism for the reaction $B_2H_3^- + CO_2$ is in good agreements with the available experimental results. The results presented in this paper may provide helpful information for understanding the chemistry of electron-deficient boron hydride anions.

Acknowledgment. This work is supported by the National Natural Science Foundation of China with the grant number 29892168.

References and Notes

(1) (a) Stock A.; Massenez, C. *Breslau Ber.* **1913**, *45*, 3539. (b) Stock, A.; Frenderici, K. *Breslau Ber.* **1913**, *46*, 1959.

(2) For excellent up-to-date reviews of boron hydride chemistry, see: (a) *Chem. Rev.* **1992**, *92*, 2. (b) *Electron Deficient Boron and Carbon Clusters*; Olah, G. A., Wade, K., Willims, R. E., Eds.; John Wiley and Sons: New York, 1991.

(3) Krempp, M.; Damrauer, R.; DePuy, C. H.; Keheyan, Y. *J. Am. Chem. Soc.* 1**994**, *116*, 3629.

(4) Van Doren, J. M.; Barlow, S. E.; DePuy, C. H.; Bierbaum, V. M. *Int. J. Mass Spectrom. Ion Processes* **1987**, *81*, 85.

(5) Nibbering, N. M. M.; Nishishita, T.; Vande Sande, C. C.; McLafferty, F. W. *J. Am. Chem. Soc.* **1978**, *70*, 45.
(6) Dunbar, R. C. *J. Am. Chem. Soc.* **1968**, *90*, 5676.
(7) Ruscic, B.; Schwarz, M.; Berkowitz, J. *J. Chem. Phys.* **1989**, *91*, 4576.
(8) Stanton, J. F.; Gauss, J.; Bartlett, R. J.; Helgaker, T.; Jorgensen, P.; Jensen, H. J. A.; Taylor, P. R. *J. Chem. Phys.* **1992**, *97*, 1211.
(9) Bigot, B.; Lequan, R. M.; Devaquet, A. *Nouv. J. Chem.* **1978**, *2*, 449.
(10) Lammertsma, K.; Ohwada, T. *J. Am. Chem. Soc.* **1996**, *118*, 7247.
(11) Frisch, M. J.; Trucks, G. W.; Schlegel, H. B.; Scuseria, G. E.; Robb, M. A.; Cheeseman, J. R.; Zakrzewski, V. G.; Montgomery, J. A.; Stratmann, Jr., R. E.; Burant, J. C.; Dapprich, S.; Millam, J. M.; A Daniels,. D.; Kudin, K. N.; Strain, M. C.; Farkas, O.; Tomasi, J.; Barone, V.; Cossi, M.; Cammi, R.; Mennucci, B.; Pomelli, C.; Adamo, C.; Clifford, S.; Ochterski, J.; Petersson, G. A.; Ayala, P. Y.; Cui, Q.; Morokuma, K.; Malick, D. K.; Rabuck, A. D.; Raghavachari, K.; Foresman, J. B.; Cioslowski, J.; Ortiz, J. V.; Stefanov, B. B.; Liu, G.; Liashenko, A.; Piskorz, P.; Komaromi, I.; Gomperts, R.; Martin, R. L.; Fox, D. J.; Keith, T.; Al-Laham, M. A.; Peng, C. Y.; Nanayakkara, A.; Gonzalez, C.; Challacombe, M.; Gill, P. M. W.; Johnson, B.; Chen, W.; Wong, M. W.; Andres, J. L.; Gonzalez, C.; Head-Gordon, M.; Replogle, E. S.; Pople, J. A. *Gaussian 98*, Revision A.6*;* Gaussian, Inc.: Pittsburgh, PA, 1998.
(12) Becke, A. D. *J. Chem. Phys.* **1993**, *98*, 5648.
(13) Pople, J. A.; Head-Gordon M.; Raghavachari, K. *J. Chem. Phys.* **1987**, *87*, 5968.
(14) (a) Gonzalez, C.; Schlegel, H. B. *J. Chem. Phys.* **1989**, *90*, 2154. (b) Gonzalez, C.; Schlegel, H. B. *J. Phys. Chem.* **1990**, *94*, 5523.
(15) (a) Reed, A. E.; Weinstock R. B.; Weinhold, F. *J. Chem. Phys.* **1985**, *83*, 735. (b) Reed, A. E.; Curtiss, L. A.; Weinhold, F. *Chem. Rev.* **1988**, *88*, 899. (c) Foster, J. P.; Weinhold, F. *J. Am. Chem. Soc.* **1980**, *102*, 7211.
(16) Rasul, G.; Surya, G. K.; Olah, G. A. *J. Am. Chem. Soc.* **1999**, *121*, 7401.